ELSEVIER

Thin Solid Films 304 (1997) 28–35

thin solid films

Growth of CdMnS films by pulsed laser evaporation

Der-San Chuu [a,*], Yu-Ching Chang [a], Cheng-Ying Hsieh [b]

[a] *Department of Electrophysics, National Chiao Tung University, Hsinchu, Taiwan*
[b] *Center of Elementary Courses, Der-Yi Nursery College, Keelung, Taiwan*

Received 4 March 1996; accepted 7 March 1997

Abstract

High orientation CdMnS thin films were grown on glass substrate by the pulsed laser evaporation (PLE) technique. Pulsed Nd:Yag laser was used as the evaporation source. During the deposition, various pulsed laser powers, substrate temperatures and different ratios of high purity CdS and MnS powder were used. X-ray diffraction (XRD), scanning electron microscopy (SEM) and energy dispersive analysis of X-rays (EDAX) were employed to study the crystal structure, surface morphology and the Mn concentration of the as-deposited films. Absorption spectra were used to investigate the band gap of CdMnS films. It was found that the deviation of the band gap of CdMnS films from that of bulk CdS at room temperature depends on the concentration of Mn. The Raman spectra of our samples showed that the mixed mode behavior of transversal (longitudinal) frequency ω^T (ω^L) might exist in the CdMnS thin films. © 1997 Elsevier Science S.A.

PACS: 75.50.Pp; 78.66.Hf; 81.15.Fg

Keywords: Pulsed laser evaporation; X-ray diffraction (XRD)

1. Introduction

Most of the diluted magnetic semiconductors (DMSs) are II–VI compounds with a fraction of the group-II constituent randomly replaced by manganese, iron, or cobalt [1,2]. These ternary alloys have attracted much attention because they permit us to tune the energy gap, the effective mass and the lattice constant by varying the concentration of the magnetic material. Furthermore, they display magnetic effects of current interests, such as the spin-glass transition, the formation of antiferromagnetic clusters and magnon excitation [3–6]. The magnetic ions in the DMS lead to a spin–spin exchange interaction between the localized magnetic moments and the band electrons [7] which results in many interesting new effects in the presence of strong magnetic fields, such as the giant Faraday rotation and the magnetic-field-induced metal-insulator transition [8–11].

Among diluted magnetic semiconductors, the Mn-based DMS can be grown over a wider composition range than Fe- and Co-based DMS [12]. Because of tunable lattice parameters and energy gaps, the Mn-based alloys are excellent candidates for fabrication of quantum wells and superlattice [13–17]. Manganese is a transition metal with valence electrons corresponding to the $4s^2$ orbital. Differing from the group-II elements, the 3d shell of the manganese is only half filled. The $4s^2$ electrons of the manganese can contribute to the $s\text{-}p^3$ bonding, and thus, can substitutionally replace the group-II elements in the II–VI alloy. In the $A_{1-x}(II)Mn_xB(VI)$ alloy, the influence of Mn on the band structure can be drastically altered provided that the Mn concentration is not very low. For example, the introduction of large mole Mn fraction may induce a change in the behavior of semimetal to semiconductor. It can also move the intrinsic edge through the visible region in wide-gap DMS. In the wide-gap materials, the localized transitions of the Mn ion dominate the optical properties at high Mn concentrations.

For wide-gap, Mn-based DMS, either zinc blend or wurtzite structure exists over a wide range of Mn concentration x. The band gap of these DMS was found to be direct. The studies of DMS were usually to investigate the optical effects because of their extremely high resistance at low temperature. In various diluted magnetic semiconductors, a nonlinear dependence of the band gap, namely, a downward bowing in the curve of band gap E_g vs. x [18],

* Corresponding author.

PII S0040-6090(97)00142-9

occurs in the region of low Mn concentration x. Such bowing is believed to arise from the nonlinear dependence of the band gap on the chemical disorder and the exchange interaction between the band carrier and the d-electron of the magnetic Mn ions.

In this work, we focus on the growth and the investigation of Raman spectra of $Cd_{1-x}Mn_xS$ thin films. This is because $Cd_{1-x}Mn_xS$ is not only the least investigated material among the Mn-based DMS, but it also manifests a pronounced bowing for low Mn concentration ($x < 0.1$) and a monotonic increase for $x > 0.1$ [19] in the curve of E_g vs. x in CdMnS single crystals. In this work, the $Cd_{1-x}Mn_xS$ thin films with various Mn concentrations were prepared at different conditions on glass substrate by pulsed laser evaporation (PLE) techniques. The structure and crystallinity of the as-deposited $Cd_{1-x}Mn_xS$ thin films were analyzed by X-ray diffraction (XRD) pattern. Raman spectra of CdS and CdMnS thin films deposited on glass substrate were investigated. Contrary to the case of the single crystal, it was found that the peak positions of main Raman vibration modes of the as-deposited $Cd_{1-x}Mn_xS$ thin films shift to higher frequency region for $x < 0.061$, while the 1LO and 2LO Raman vibration modes split into two modes for $x > 0.061$.

This paper will be organized as follows: the experimental procedures will be described in detail in the next section, results and discussions will be presented in Section 3 and a short conclusion will be given in the final section.

2. Experimental

$Cd_{1-x}Mn_xS$ thin films were prepared by PLE techniques. The laser deposition system was evacuated by a turbo-molecular pump (ALCATEL, type 5081) and a mechanical pump (ALCATEL 2010 pascal rotary pump). A pirani and a cold cathode (penning) gauge were used to measure the total pressure of the vacuum chamber. The base pressure of this system was less than 6.0×10^{-6} Torr. In the process of evaporation, the pressure was kept at about 1×10^{-5} Torr. Two thermocouple-electrical feedthroughs were used to connect the rotary instruments and heater inside the vacuum chamber. The target holder was connected with a rotary motor which can make the laser beam irradiate the target holder over a wider area instead of focusing on the same point during the whole evaporation process. The substrate was heated by a tantalum resistance wire. The heating current was controlled by an autotransformer. The current range was kept from 0 to 15 A, which can make the substrate achieve temperatures from room temperature to 300°C. The temperature of the substrate was controlled by a thermal controller. The distance between the target and the substrate was kept at about 30 mm.

The pulsed Nd:Yag laser with harmonic generators was operated at a repetition rate of 4 pulses/s with a pulsed energy of ~ 18 mJ/pulse and a duration time of 8×10^{-9} s. The emitted wavelengths of the laser were 1064 nm, 532 nm and 355 nm. Two of these emitted wavelengths were used during the evaporation. One was 1064 nm and the other was a mixture of 1064 nm and 532 nm. The laser beam diameter at source was 7 mm with a divergence of 0.5 mrad. The laser energy was about 5 mJ–25 mJ/pulse. The laser beam was filtered through the quartz window and then was focused on the target which was rotated in a vacuum chamber. The material was evaporated perpendicularly to the target surface. The targets were formed by mixing pure (99.999%) CdS and MnS powder. The powder was mixed in various ratio in order to obtain a different concentration of Mn. After competent mixed and comminuted, all of the powder were pressed into a pellet. $Cd_{1-x}Mn_xS$ films were deposited on Corning's 7059 glass slices at 250°C–260°C substrate temperature. The typical deposition rate was ~ 0.3 Å/s. The color of the CdS thin films was found to be orange-yellow, the MnS thin films were deep-gray and the CdMnS thin films were intervenient.

The crystallinity and surface morphology were identified by XRD and scanning electron microscopy (SEM). The films were prepared with a thickness of ~ 1000 Å to 3000 Å. The thickness of the thin films was measured by the ellipsometer with an accuracy of within 10 Å. (Autoel-III, the incident light is the 6328 Å line of He–Ne Laser, 4.1 mW maximum linearly polarized, 0.075 mW maximum elliptically polarized, incident angle is 70°, the standard errors of ellipsometric parameters ψ and Δ are 0.005 and 0.02, respectively). The concentrations x of Mn in the $Cd_{1-x}Mn_xS$ thin films were studied by energy dispersive analysis of X-ray (EDAX). The absorption spectra for probing the band structure were investigated by a double grating monochromator (SPEX 1404), in which the spectral coverage was from 175 nm to 1040 nm. A range of 350 nm–750 nm was used to observe the spectra. The light source was a Quartz-Tungsten-Halogen (QTH) lamp (ORIEL 10–250 watt QTH source). The white light was filtered through the sample and was collected by the monochromator. The signals were detected by an R928 photomultiplier (PMT). The monochromator and PMT were controlled by a computer (286 PC). The absorption coefficient α was obtained by calculating and normalizing the transmission through the sample to the transmission through a clean substrate (glass). Raman spectra without polarization analysis were recorded by a back-scattering spectroscopy arrangement. The 4880 Å line of Ar^+ laser was used as an excitation source for the Raman experiment. Spectra were taken at room temperature in the 45° reflection geometry with the sample being placed under the micrometer stage of a triple grating spectrograph (Spex 1877C) equipped with liquid nitrogen cooled CCD detectors array (Photometrics CC200). The arrangement of triple grating monochromator was used. The incident power of

the laser on the sample was about 100 mW. The scattering light was focused by camera lens into the slit of triple grating spectrograph. The slit widths used led to a resolution of 1 cm^{-1}.

3. Results and discussion

The structure and crystallinity of the as-deposited $Cd_{1-x}Mn_xS$ thin films were analyzed by XRD method which employed filtered Cu $K\alpha$ radiation ($\lambda = 1.5418$ Å). Fig. 1 shows the XRD results of the films deposited by PLE technique on a glass substrate of 9 mJ, 12 mJ, 15 mJ, 18 mJ and 21 mJ/pulse with the wavelength of 1064 nm mixed with 532 nm. The intensity of XRD peaks is stronger when laser energy with 15 mJ/pulse and 18 mJ/pulse was used. Fig. 2 shows the variance of the XRD peak intensity on different laser energies as the pure 1064 nm wavelength of the Nd:Yag laser was used as the evaporation source. It can be seen from the figure that the strongest peak can be accrued when a percentage of 18 mJ/pulse laser energy was used. The other depositing conditions were the same for Fig. 1 and Fig. 2: (1) the targets used were 0.46 g CdS powder mixed with 0.23 g MnS powder ($x = 0.454$); (2) the repetition rate of the laser pulse is 4 pulses/s; (3) deposition time is 60 min; (4) substrate temperature is 250°C. From Fig. 1 and Fig. 2, it can be noted that all the XRD peaks of $Cd_{1-x}Mn_xS$ thin films are about 26.4°–27.5° (2θ), and are similar to the value of 26.3° of the (002) orientation of CdS as shown in the inset of Fig. 3. That is the orientation of wurtzite structure. Since the structure of our films was determined solely on the position of the peak in the XRD pattern, the films, therefore, may have a texture structure corresponding to the (002) orientation of the wurtzite structure. It can also be noted that the locations of XRD peaks shown in Fig. 1 and Fig. 2 are somewhat different for different laser

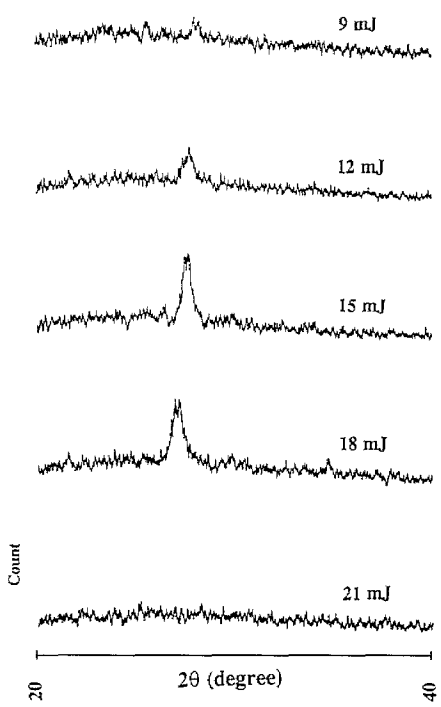

Fig. 1. The XRD patterns of the as-deposited films prepared by PLE technique used laser energy of 9 mJ, 12 mJ, 15 mJ, 18 mJ and 21 mJ/pulse with a wavelength of 1064 nm mixed with 532 nm. The targets were 0.46 g CdS mixed with 0.23 g MnS.

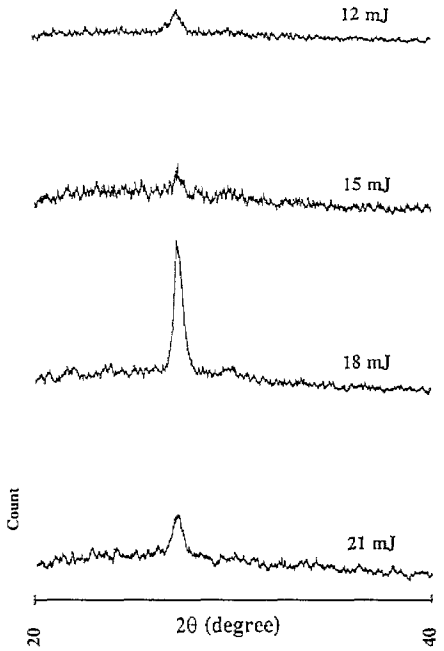

Fig. 2. The XRD patterns of the as-deposited films prepared by PLE technique used laser energy of 12 mJ, 15 mJ, 18 mJ and 21 mJ/pulse with a wavelength of 1064 nm. The targets were 0.46 g CdS mixed with 0.23 g MnS.

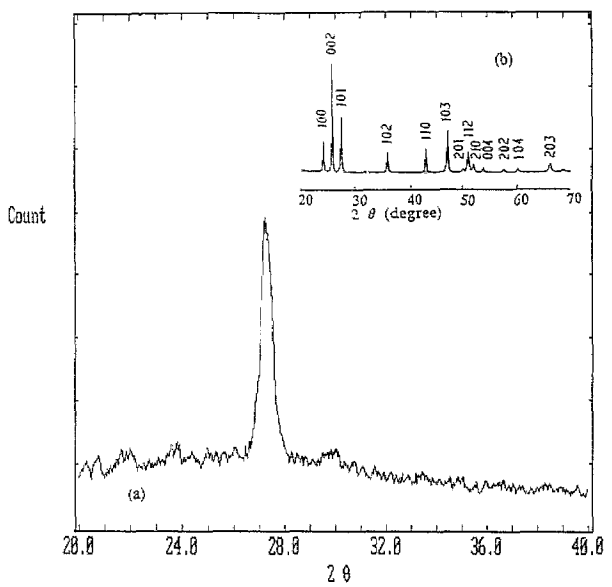

Fig. 3. (a) The XRD pattern of the as-deposited CdMnS films prepared by PLE technique; (b) XRD pattern of CdS powder.

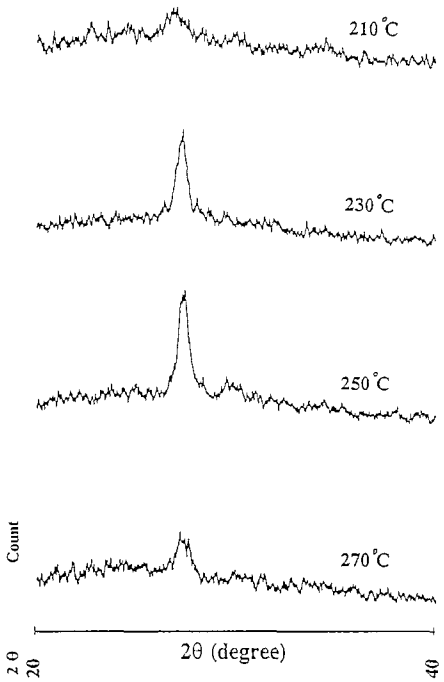

Fig. 4. The XRD patterns of the as-deposited films prepared by PLE technique at substrate temperature of 210°C, 230°C, 250°C and 270°C. The targets were 0.46 g CdS mixed with 0.23 g MnS.

energies and laser wavelengths. The shift of the peaks may be ascribed to the partial substitution of Cd by the Mn. Although all the targets used for the production of the films in Fig. 1 and Fig. 2 were the same, our results, however, manifested that the Mn concentrations x contained in $Cd_{1-x}Mn_xS$ thin films depend on the laser energy and the laser wavelength used in the evaporation.

In the following, we will concentrate on the $Cd_{1-x}Mn_xS$ thin films deposited by using a laser energy of 18 mJ/pulse with a wavelength of 1064 nm. In Fig. 4, different substrate temperatures were used in the deposition of thin films while the other deposition parameters (e.g., the film thickness and area and the deposition time) were kept the same. The target materials were the same as those used in Fig. 1 and Fig. 2. It can be seen from Fig. 4 that a stronger XRD peak can be attained when the substrate temperature is kept at 250°C.

The surface morphology of the as-deposited films studied by SEM is shown in Fig. 5. Fig. 5(a) shows the SEM photograph of the CdS thin film; Fig. 5(b) that of MnS thin film; Fig. 5(c) that of $Cd_{1-x}Mn_xS$ thin film which was deposited by evaporating the target of 0.46 g CdS powder mixed with 0.23 g MnS powder; and Fig. 5(d) is the photograph of $Cd_{1-x}Mn_xS$ thin film with $Cd_{1-x}Mn_xS$

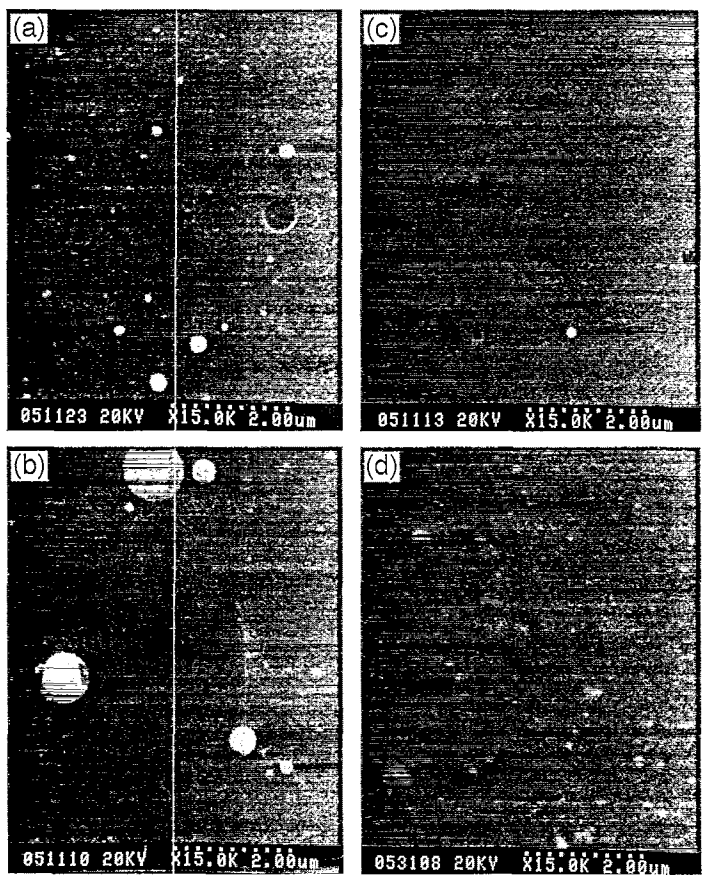

Fig. 5. The SEM photographs of the films grown on glass substrate by PLE technique. The targets were (a) CdS powder; (b) MnS powder; (c) 0.46 g CdS mixed with 0.23 g MnS powder; and (d) $Cd_{1-x}Mn_xS$ single crystal with $x = 0.0173$.

single crystal ($x = 0.0173$) as the target. The surfaces of these films were found to be smooth optically and adhered firmly to the substrate. However, there were a few whitish small spots adhered to the surface of the films. These particulates or precipitates were produced by spurting from the target and directly amassed in the films. The composition of these particulates is very close to that of the target. It can be noted from Fig. 5 that the $Cd_{1-x}Mn_xS$ thin film, which was deposited by evaporating the target of the mixture of CdS and MnS powder, has the cleanest surface with only very few spurting particulates on the surface. The grain sizes of $Cd_{1-x}Mn_xS$ films were estimated by using the FWHM of the XRD peaks and were found to be in an average of ~ 300 Å.

The Mn concentrations x in the $Cd_{1-x}Mn_xS$ thin films were studied by EDAX. Table 1 shows the concentrations of as-deposited films that were measured by EDAX and the Mn concentration contained in the targets. These films were deposited on the glass substrate at 250°C. The excitation source was the 1064 nm line of Nd:Yag laser. In the EDAX measurements of thin films, a single crystal $Cd_{1-x}Mn_xS$ was used as the standard. Because the films have a high resistance, we must coat Au on the film surface for the EDAX measuring. That made the signals of S and Au overlap. Therefore, we can analyze the concentration of Mn and Cd only. The data of EDAX were taken over the film surface and thus included the spurting particulates which have a slightly smaller Mn concentration. Since the number of particulates were very few compared with the rest of the area of the thin film, the deviation of the measuring concentration x of Mn was, therefore, believed to be small and may be less than $0.05x$–$0.1x$. This can be confirmed by calculating the lattice constant of the $Cd_{1-x}Mn_xS$ thin films. The lattice constant c along the c-axis of the $Cd_{1-x}Mn_xS$ thin films can be obtained using the equations: $2d \sin\theta = n\lambda$ and $d = c/[h^2(a/c)^2 + k^2(a/c)^2 + l^2]^{1/2}$, where $(hkl) = (002)$. The calculated lattice constants of $Cd_{1-x}Mn_xS$ thin films for various x were found to decrease linearly as x was increased and were within the experimental error with the linear dependence of the bulk lattice constant on x which can be obtained by using the lattice constants of CdS and MnS from the handbook. Thus, the accuracy of the Mn concentration x determined from EDAX should be acceptable. In Table 1, it can be noted that the Mn concentrations of the films were, in general, higher than those of the targets. This might be due to the relatively low vaporization temperature of sulphur. As shown in previous works [20a,20b], the concentration of Mn in $Cd_{1-x}Mn_xS$ was usually in the range of $0 \le x \le 0.5$. Thus, our EDAX results seem to be consistent with previous results.

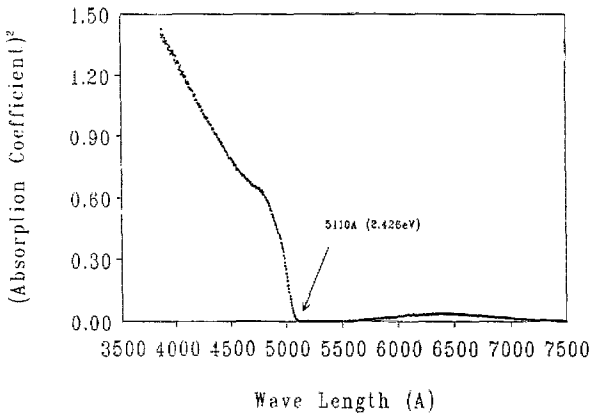

Fig. 6. Absorption spectrum of the CdS thin film deposited by PLE technique.

Fig. 6 is the relationship of α^2 (α is the absorption coefficient) and h_ν (photon energy of incident light) by measuring I (transmitted light intensity) and I_0 (incident light intensity). The band gap of CdS thin films obtained was about 2.426 eV which is very close to the value of 2.42 eV of CdS bulk at room temperature. The blue shift of the band gap of thin films might be ascribed to the size effect of the small grains. From the absorption spectra, we obtained the band gap of the as-deposited CdMnS thin films as those listed in Table 2. The band gaps of CdMnS films can be higher or lower than that of bulk CdS, which depends on the value of the concentration x. Compared to the previous result of Ikeda et al. [19], it can be concluded that in our sample, Mn has been set in the CdS structure. Fig. 7 shows the variation of the energy gap E_g of $Cd_{1-x}Mn_xS$ versus the Mn concentration x. In this figure, it can be observed that the bowing characteristics of the band gap versus x of our sample were similar to the results obtained by Ikeda et al. [19]. However, the Mn concentration x, where the minimum of the band gap occurs, was different for thin films and single crystals. It was known that the chemical disorder is the only source

Table 1
The concentration of Mn in the as-deposited films measured by EDAX compared with the targets

Mn concentration in target	Mn concentration x of thin film from EDAX
0.0574	0.1229
0.0301	0.061
0.0063	0.0176
0.0	0.0

Table 2
Band gap of the as-deposited films measured by absorption measurement

E_g (eV)	Mn concentration x measured from EDAX
2.403	0.0176
2.416	0.061
2.426	0.000
2.447	0.094
2.463	0.1229
2.570	0.242

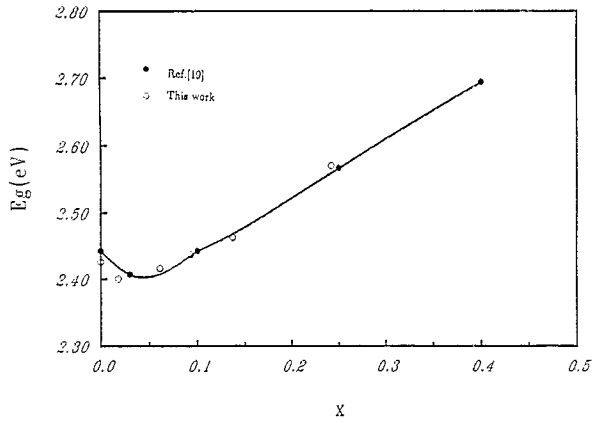

Fig. 7. Variations of energy gap with Mn concentration x in the as-deposited films compared with the results of Ref. [19].

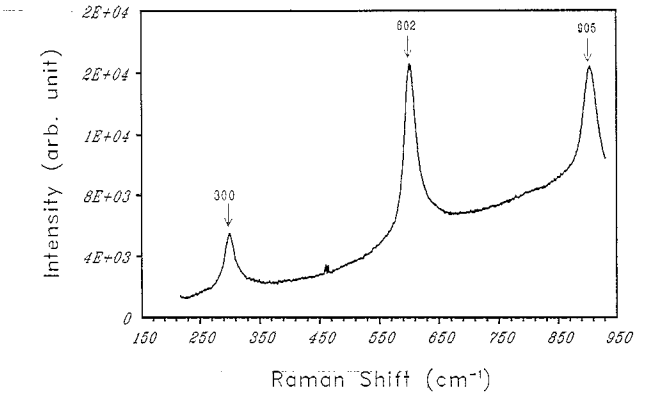

Fig. 8. Raman spectrum of the CdS thin film deposited by PLE technique.

for band bending of nonmagnetic semiconductors [21], while the exchange interaction between the carrier and the magnetic ions is the other possible source for band bending in the diluted magnetic semiconductors. Since the size of the grain of $Cd_{1-x}Mn_xS$ thin films depends on the Mn concentration x and, thus, might have an effect on the exchange interaction constants, which also depend on the value of x. The slight difference in the effect of the exchange interaction between the carrier and the magnetic ions on the conduction and valence bands for thin films and single crystals might cause the shift of the minimum of the curve of the band gap versus x.

Fig. 8 shows the Raman spectrum of CdS thin film deposited on the glass substrate. The excitation source was the 4880 Å line of Ar^+ laser. The spectrum shows that the 1LO Raman peak of the as-deposited film was located at ~ 301 cm^{-1}, 2LO at ~ 602 cm^{-1} and 3LO at ~ 901 cm^{-1}. The 1LO phonon shift of CdS crystal was given in the literatures [22,23] as 305 cm^{-1} (bulk). The position of the 1LO phonon peak of Raman scattering spectrum of CdS thin film measured by Scott and Damen [24] was 300 cm^{-1}. The decrease in the LO phonon energy was attributed to the lattice softening of the CdS thin film due to the reduced dimension of the thin film. The Raman shift of the surface modes of the microcrystallites in CdS film reported by Chuu et al. [25] is 296 cm^{-1}. Our data is close to the result obtained by Scott and Damen. In the case of the $Cd_{1-x}Mn_xS$ thin film in our result, two phenomena can be observed when Mn ions were contained in thin films of CdS structure. Fig. 9(a) shows a shift in peak position (one-mode behavior) and Fig. 9(b) shows a peak splitting into two peaks (two-mode behavior). The spectra of $Cd_{1-x}Mn_xTe$ have been studied in considerable detail [26]. Due to the significant difference in the masses of Cd and Mn, the optical phonons of this alloy exhibited what was known as two-mode behavior; in addition, intense disorder-induced features were also observed in its Raman spectrum. The two-mode behavior also displayed in $Cd_{1-x}Mn_x$ [27]. The optical phonons of $Zn_{1-x}Mn_xTe$, $0.003 \leq x \leq 0.7$, display a behavior that was mixed-mode intermediate of the one-mode and two-mode cases [28]. For the $Cd_{1-x}Mn_xS$ bulk crystal published by Suh et al.

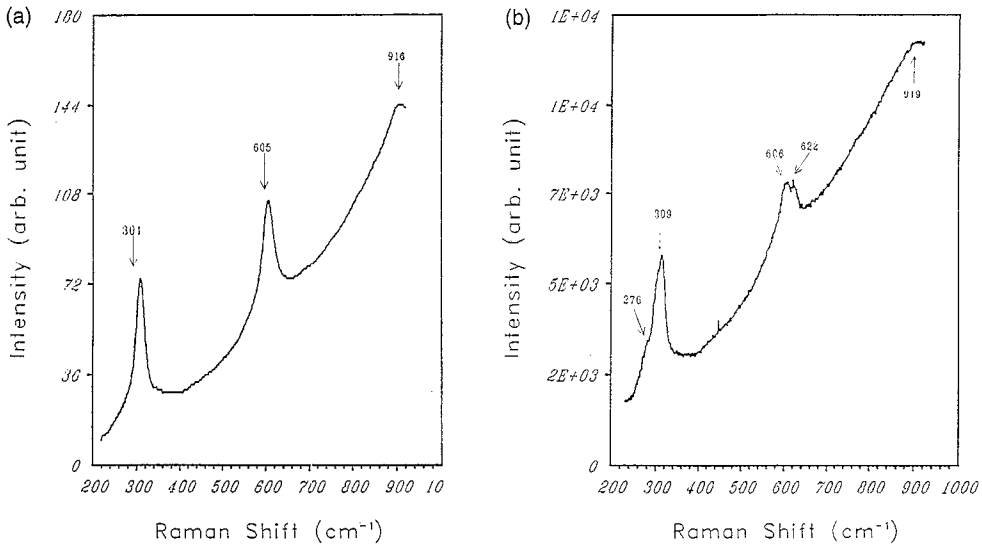

Fig. 9. Raman spectrum of the as-deposited $Cd_{1-x}Mn_xS$ thin film with Mn concentration (a) $x < 0.061$; (b) $x \geq 0.061$.

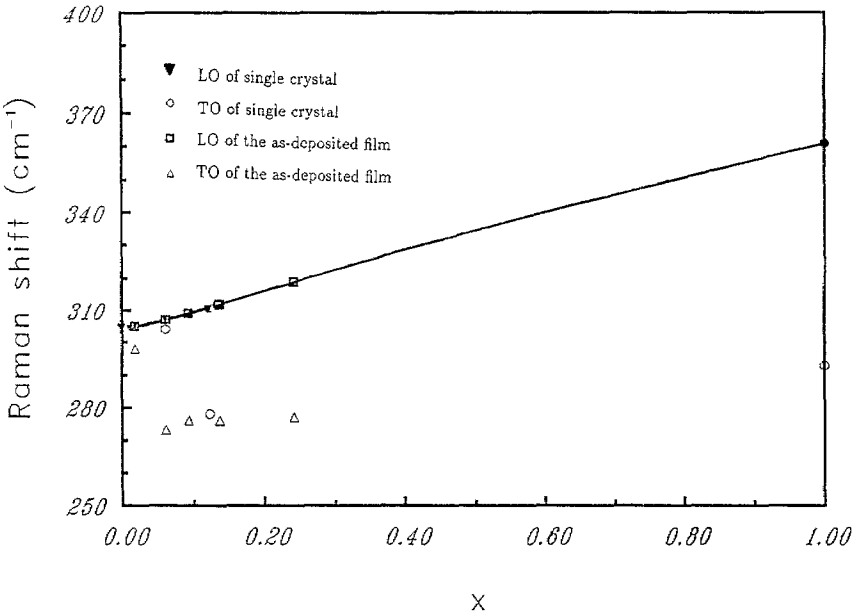

Fig. 10. Shifts of Raman peaks of the as-deposited $Cd_{1-x}Mn_xS$ films.

[27], a mixed-mode behavior intermediate of the one-mode and two-mode behavior can be observed. Fig. 9 shows that a mixed-mode behavior seems also to exist in $Cd_{1-x}Mn_xS$ thin films. It can be observed that the position of Raman peak exhibits blue shift behavior for the Mn concentration $x < 0.061$, while the position of Raman peak shows splitting behavior for the Mn concentration $x \geq 0.061$. The possible reason for this result may be explained as follows: As the Mn concentration x was increased from 0 to 0.061, the lattice constant c was decreased due to the smaller atomic size of Mn than that of Cd. This resulted in an increase in the phonon frequency. While the Mn concentration x was increased to become larger than 0.061, the LO phonon splits into two peaks because the MnS-like phonon appears. As a result, we have blue shift behavior for $x < 0.061$ and mode splitting behavior for $x \geq 0.061$. The splitting of the phonon modes might be attributed to the strain between the substrate and the thin film; however, the thickness of our films was ~ 2000 Å in average and the lattice constants c for these films were very close to that of the bulk. Thus, with such a thickness the strain between the substrate and the thin film might be released. Therefore, to investigate the strain effect on the Raman shift, thinner films must be grown; however, the thinner the film, the worse the film quality.

Fig. 10 shows the phonon frequency dependence on x of our $Cd_{1-x}Mn_xS$ thin films. For comparison, we also included the results of the $Cd_{1-x}Mn_xS$ single crystals which were grown by the temperature gradient solution method in our laboratory. It can be observed that the variation of Raman shift of LO phonon modes with the concentration of Mn was very similar for both thin films and single crystals while the variation of the Raman shift of TO phonon modes was somewhat different for thin films and single crystals. It can also be observed that the LO phonon energy exhibits a blue shift compared to the 301 cm^{-1} of 1LO Raman peak of our as-deposited CdS film as some of the Cd atoms are substituted by Mn atoms.

4. Conclusion

PLE technique was used to grow the CdMnS thin films on the glass. Different laser energies, substrate temperatures and target materials were used in this work. The results of XRD showed that the films obtained were highly oriented in (002) direction. From the results of EDAX, assignment of the quantify of the Mn concentration in the films was made. In the absorption measurement, we found that the band gap of the films varied with the Mn concentration x. That can be ascribed to the fact that Cd was substituted by Mn in the CdS's structure. The Raman spectra of our sample showed that the blue shift of the peak position of Raman spectra for thin films occurred compared with the bulk sample for Mn concentration $x < 0.061$, while the peak splitting existed for $x \geq 0.061$. Our thin CdMnS films also exhibited bowing behavior, which was shown in the CdMnS single crystal, for low concentration x as the E_g was plotted versus x, although the minimum position of the curve of E_g versus x was different for thin films and single crystal.

Acknowledgements

This work is supported partially under grant number NSC 86-2112-M-009-06 by the National Science Council, Taiwan, R.O.C.

References

[1] N.B. Brandt, V.V. Moshchalkov, Advances in Physics 193 (1984) 33.
[2] J.K. Furdyna, J. Appl. Phys. 7637 (1982) 53.
[3] S.B. Oseroff, Phys. Rev. B25 (1982) 6584.
[4] T. Dolling, T.M. Holden, V.F. Sears, J.K. Furdyna, W. Giriat, J. Appl. Phys. 53 (1982) 7644.
[5] A.K. Ramdas, J. Appl. Phys. 53 (1982) 7649.
[6] A. Twardowski, Phys. Scripta T39 (1991) 124.
[7] A.J. Gaj, J. Phys. Soc. Jpn., 49, Suppl. A (1980) 797.
[8] E. Oh, A.K. Ramdas, J.K. Furdyna, J. Lumin. 52 (1992) 183.
[9] J. Frey, R. Frey, C. Flytzanis, Phys. Rev. B45 (1992) 4056.
[10] M. Kohl, D.D. Awschalom, J. Appl. Phys. 70 (1991) 6377.
[11] P.A. Wolff, J. Warnok, J. Appl. Phys. 55 (1984) 2300.
[12] J. Mukesh (Ed.), Diluted Magnetic Semiconductors, World Scientific, Singapore, 1991.
[13] B.T. Jonker, X.C. Liu, W.C. Chou, A. Petrou, J. Warnock, J.J. Krebs, G.A. Prinz, J. Appl. Phys. 69 (1991) 6097.
[14] B.T. Jonker, W.C. Chou, A. Petrou, J. Warnock, J. Vac. Sci. Technol. A14 (1992) 1458.
[15] N. Samarth et al., J. Vac. Sci. Technol. B10 (1992) 915.
[16] W.C. Chou, A. Petrou, J. Warnock, B.T. Jonker, Phys. Rev. B46 (1992) 4316.
[17] W.C. Chou, A. Petrou, J. Warnock, B.T. Jonker, Phys. Rev. Lett. 67 (1991) 3820.
[18] A.G. Thompson, J.C. Woolley, Can. J. Phys. 45 (1967) 255.
[19] M. Ikeda, H. Itoh, H. Sato, J. Phys. Soc. Jpn. 25 (1968) 455.
[20a] W.R. Cook, J. American Ceramic Society 51 (1968) 518.
[20b] D.R. Yoder-Short, U. Debska, J.K. Furdyna, J. Appl. Phys. 58 (1985) 4056.
[21] A. Zunger, J.E. Jaffe, Phys. Rev. Lett. 51 (1983) 662.
[22] M.V. Klein, S.P.S. Porto, Phys. Rev. Lett. 22 (1969) 782.
[23] J.F. Scott, R.C.C. Leite, T.C. Damen, Phys. Rev. 188 (1969) 1285.
[24] J.F. Scott, T.C. Damen, Opt. Commun. 5 (1972) 410.
[25] D.S. Chuu, C.M. Dai, W.F. Hsieh, C.T. Tsai, J. Appl. Phys. 69 (1991) 8402.
[26] S. Venugopalan, A. Petrou, R.R. Galazka, A.K. Ramdas, S. Rodriguez, Phys. Rev. B25 (1982) 2681.
[27] E.K. Suh, A.K. Arora, A.K. Ramdas, S. Rodriguez, Phys. Rev. B45 (1992) 3360.
[28] D.L. Peterson, A. Petrou, W. Giriat, A.K. Ramdas, S. Rodriguez, Phys. Rev. B33 (1986) 1160.